Hindawi
International Journal of Photoenergy
Volume 2021, Article ID 6648325, 12 pages
https://doi.org/10.1155/2021/6648325

Research Article

Biotemplated Synthesis of Titanium Oxide Nanoparticles in the Presence of Root Extract of *Kniphofia schemperi* and Its Application for Dye Sensitized Solar Cells

Eneyew Tilahun Bekele,[1] **Enyew Amare Zereffa**,[1] **Noto Susanto Gultom**,[2] **Dong-Hau Kuo**,[2] **Bedasa Abdisa Gonfa**,[1] **and Fedlu Kedir Sabir**[1]

[1]*Department of Applied Chemistry, School of Applied Natural Science, Adama Science and Technology University, P.O. Box 1888, Adama, Ethiopia*
[2]*Department of Materials Science and Engineering, National Taiwan University of Science and Technology, No. 43, Sec. 4, Keelung Road, Taipei 10607, Taiwan*

Correspondence should be addressed to Bedasa Abdisa Gonfa; bedassa.abdissa@astu.edu.et
and Fedlu Kedir Sabir; fedluked130@gmail.com

Received 17 November 2020; Accepted 8 February 2021; Published 20 February 2021

Academic Editor: Kei Ohkubo

Metal oxide nanoparticles prepared by biological route using green plant parts as a template are eco-friendly as well as yield good results than the conventional methods. This present study focusses on biosynthesis and characterization of TiO_2 NPs using root extract of *Kniphofia schemperi* for dye-sensitized solar cells. TiO_2 NPs were synthesized using 0.25 M titanium tetra butoxide in the presence of root extract of *Kniphofia schemperi* with the volume ratios. The analysis result revealed that the synthesized TiO_2 NPs were thermally stable above 500°C and have spherical morphology, with the average crystalline size of 11.7, 8.3, and 8.6 nm, and band gap energy of 3.35 eV, 3.33 eV, and 3.36 eV, respectively, for the TiO_2 NPs prepared at the volume ratios of 2 : 3, 1 : 1, and 3 : 2. Biosynthesized TiO_2 NPs were used as photoanode in dye-sensitized solar cells (a device used for converting absorbed light into electricity). Solar cell devices were fabricated using roots of *Kniphofia schemperi* sensitizer in the presence of TiO_2 NPs biosynthesized within (2 : 3, 1 : 1, and 3 : 2) volume ratio, which showed power conversion efficiency of 0.039%, 0.117%, and 1.3%. Incident photon to current conversion efficiency (IPCE) analysis using TiO_2 (2 : 3, 1 : 1, and 3 : 2) photoelectrodes showed 6.64%, 2.66%, and 18%. Among the biosynthesized TiO_2 different volume ratios, TiO_2 (3 : 2) NPs showed relatively maximum solar cell efficiency and IPCE value due to its uniform spherical shape that enables to absorb large dye molecules on its surface, and this intern improves device efficiency.

1. Introduction

Energy exists in different forms from burning woods to obtain fire in prehistoric times to electricity productions in the modern age. Its consumption is one of the most important aspects in everyday life activities of human beings. However, the original sources of energy that peoples used to harvest have shown signs of deficiency due to the rapid growth in industrialization in many countries. As a result, increasing concerns about energy crisis, climate change, shortage in fossil fuels, and environmental issues are motivating the researcher to develop clean, sustainable, and renewable energy resources that will power the future [1].

Recent advances in solar energy conversion technologies based on organic semiconductors as light harvesting layer employ metallic oxide semiconductor (MOS) nanostructures for efficient charge extraction and transportation between the electrode and organic molecules [2]. Solar cells based on

dye-sensitized and porous nanocrystalline TiO_2 photoanode with attractive performance were first reported in 1991 [3]. Dye-sensitized solar cell (DSSC) is a low-cost cell and belongs to the group of thin film solar cells. The interconnected TiO_2 NP in DSSCs has been widely used as the mesoporous electrode film layer, because it is beneficial for light adsorption with a large amount of dye molecules due to its large surface areas [4].

TiO_2 NPs have been routinely synthesized by several approaches such as hydrothermal, solvothermal, sol-gel, direct oxidation, chemical vapor deposition, electro-deposition, sonochemical, chemical bath deposition, and microwave methods [5]. However, these methods are costly, toxic, not friendly to the natural ecosystem. Nowadays, there is an increased demand to develop TiO_2 with high yielding, low cost, and nontoxicity by exploring with biological sources and eco-friendly methods. The biological method involves the use of environment-friendly materials such as plant extracts (leave, flower, bark, root, seed, and peels), bacteria, fungi, and enzymes in the synthesis of titanium dioxide nanoparticles together with the use of green solvents [6].

The species *Kniphofia* are herbaceous perennials growing from rhizomes. *Kniphofia schemperi* is also known as *Kniphofia schemperi baker*; its root has been traditionally applied for the treatment of various diseases such as menstrual pains, abdominal cramps, intestinal tape worm, wounds, dysmenorrheal, bacterial, and fungal infections, malaria, chest complaint, and gonorrhea, and hepatitis B [7]. Furthermore, the presence of various functional groups within the root extract of *Kniphofia schemperi* such as flavonoids, carbonyl groups, carboxylic acids, ketones, and phenols could be used for the synthesis of TiO_2 nanoparticles in order to avoid the use of toxic and expensive chemical species for the synthesis process. The root extract of the plant with same family name, *Kniphofia foliosa*, has been used for synthesis of TiO_2 NPs for antibacterial activity by Eneyew et al. [8]. And under this work, the root extract of *Kniphofia schemperi* was investigated as a template for the synthesis of TiO_2 NPs and also could be used as a natural sensitizer for solar cell application.

DSSCs using inorganic complex dyes and commercially available and chemically synthesized TiO_2 NPs have been explored and its corresponding performance is also measured. But titanium oxide nanoparticles are not produced using a biosynthesized and eco-friendly method for DSSCs applications as photoanode using root extract of *Kniphofia schemperi* [9]. To the knowledge of different researchers, green synthesis of TiO_2 NPs using indigenous medicinal plant extract from the root of *Kniphofia schemperi* for DSSCs application is not done yet. Therefore, the focus of the current work was biosynthesis of TiO_2 NPs in different volume ratios using titanium tetra butoxide and *Kniphofia schemperi* root extract as a reducing and capping agent and then to fabricate DSSCs using sensitizers obtained from root of *Kniphofia schemperi*. In the present findings, the root extract of *Kniphofia schemperi* was played two roles, in one case used as a capping and reducing agent for TiO_2 biosynthesis, and in the second case, it was used as a sensitizer during photoanode preparation to coat the prepared film.

2. Methodology

2.1. Chemicals and Reagents. Chemicals and reagents used in this work were titanium tetra butoxide (Acros organics, 98%), acetone (Sigma Aldrich), acetonitrile (Sigma Aldrich), sodium hydroxide (Sigma Aldrich), iodine crystal (Sigma Aldrich), NaI (BDH), 1-ethyl-3-methyl immidazolium iodide (EMIMM-I: Sigma Aldrich), isopropanol (Riedel-de Haen), PVP (Sigma Aldrich), $(C_2H_5)_4NBF_4$ (Sigma Aldrich), (ethylenedioxythiophene) (EDOT, Sigma Aldrich), absolute ethanol (Lab Tech Chemicals), triton X-100 (Sigma Aldrich), and conductive FTO glass substrate (Sigma Aldrich). All the chemicals and reagents were of analytical grade and used without further purification.

2.2. Extraction of Root of Kniphofia schemperi. Healthy and fresh roots of *Kniphofia schemperi* were collected and cleaned using distilled water several times and were dried in a shaded room till all the moisture content of the roots were removed. The dried *Kniphofia schemperi* root was ground using plant grinding machine. The extraction process was performed by mixing 15 grams of powder of the root with 250 mL of absolute ethanol in a 500 mL erlenmeyer flask. And then, the mixture was allowed to boil at 50°C for about one hour. The extracted solution was collected and stored at 4°C within a refrigerator [10]. The filtrate of the extract was used as a capping and reducing agent for the biosynthesis of TiO_2 NPs within three different volume ratios.

2.3. Biosynthesis of TiO_2 NPs Using Root of Kniphofia schemperi. TiO_2 NPs were biosynthesized by using 0.25 M of the precursor Titanium tetra butoxide, $C_{16}H_{36}O_4Ti$, and ethanolic root extract of *Kniphofia schemperi* of different volume ratios: 2 : 3 (40 mL precursor salt versus 60 mL of root extract of *Kniphofia schemperi*), 1 : 1 (50 mL precursor salt versus 50 mL root extract of *Kniphofia schemperi*), and 3 : 2 (60 mL precursor salt versus 40 root extract of *Kniphofia schemperi*). The prepared NPs were labeled as TiO_2 (2 : 3), TiO_2 (1 : 1), and TiO_2 (3 : 2). All solutions of different volume ratios were stirred for about five hours without heating. The precipitated was formed by drop wise addition of solution of sodium hydroxide as a precipitating agent. The solution with a precipitate was centrifuged at 1000 rpm and washed four times with distilled water and absolute ethanol, dried in oven overnight at 100°C, and calcined at 500°C for about four hours [10]. Figure 1 shows the schematic synthesis process of TiO_2 NPs using root extract of *Kniphofia schemperi* and from its titanium tetra butoxide precursor.

2.4. Characterizations of Biosynthesized TiO_2 NPs. Thermal gravimetric analysis was carried out using a TGA/DTA (DTG-60H Shimadzu Co., South Korea) to determine the calcination temperature of TiO_2 NPs. The infrared spectroscopy FTIR (PerkinElmer 65) was used to identify functional groups of biosynthesized TiO_2 NPs [11–13]. The crystalline structure of the biosynthesized TiO_2 NPs was investigated by X-ray diffraction using X-ray diffractometer (XRD (XRD-7000, Shimadzu Co., South Korea). The UV-Vis absorption spectrum of biosynthesized TiO_2 NPs was confirmed using UV-Vis spectrophotometer (JASCO V-670)

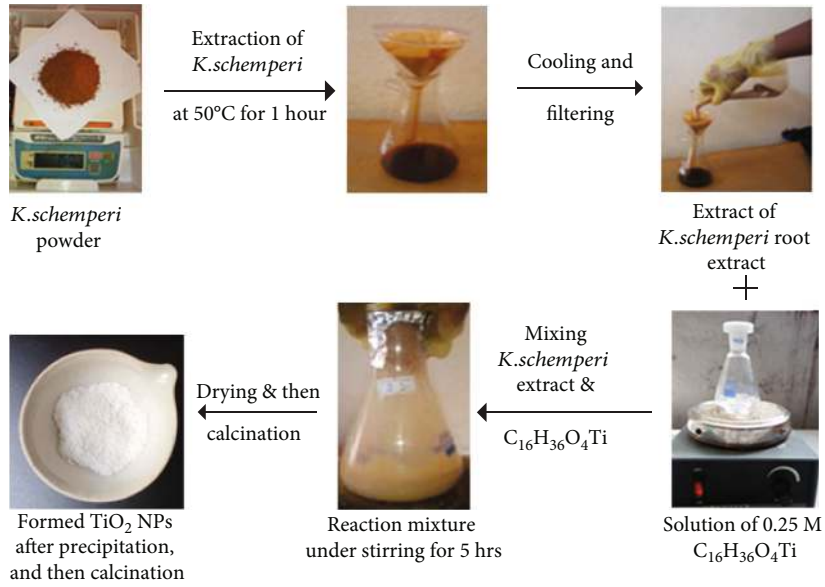

Figure 1: Schematic biosynthetic procedure of TiO_2 NPs using root extract *Kniphofia schemperi*.

with scan wavelength of 200 to 800 nm [14–16]. The morphology and microstructure of biosynthesized TiO_2 NPs were observed using field emission SEM-EDS (FE-SEM, JEOL-JSM 6500F, Japan) and high-resolution TEM (HRTEM, Tecnai F20 G2, Philips, Netherlands).

2.5. Extraction and Preparation of Sensitizer. Roots of *Kniphofia schemperi* were collected from Bale National Park, Oromia regional state, Ethiopia. Those collected samples were surface cleaned repeatedly and allowed to dry under shadow at room temperature. Then, it was ground into powder and packed in a plastic bottle by covering with aluminum foil and storing it in a dark area. The extract was obtained by taking 4 g powders of roots of *Kniphofia schemperi* to be socked in an erlenmeyer flask with 100 mL of absolute ethanol. The mixture solution was placed in a dark place and covered with aluminum foil to avoid photooxidation. The solution was stored for about 24 h at room temperature until the required pigment solution was extracted. Then, the solid materials were hold still overnight, and the clear solution of the dye was obtained. The clear solution to be used for sensitization purpose was separated from solid materials using glass filters [17, 18].

2.6. Fabrication Steps of DSSCs

2.6.1. Preparation of the Substrate for Deposition. The conductive fluorine-doped tin oxide (FTO) glass substrate with an area of 2 cm × 2.5 cm was cleaned repeatedly with distilled water and acetone, isopropanol, and ethanol sequentially under ultrasonication for about 20 minutes in each different solvent in order to remove organic and inorganic dirts from the surface of the substrate. The substrates were thoroughly cleaned before deposition of films of biosynthesized TiO_2 (2 : 3, 1 : 1, and 3 : 2) NPs was carried out.

2.6.2. Semiconductor Oxide Material Paste Preparation and Deposition. TiO_2 paste was prepared according to the method developed by Nazeeruddin et al. [19]. As an example, 0.76 g powder from each kind of TiO_2 volume ratio was ground in a porcelain mortar with a drop-wise addition of 1 mL of H_2O containing 0.56 mL of 1 M HNO_3 to prevent reaggregation. After the powder had been dispersed by the high shear forces in the viscous paste, it was diluted by additional drop-wise of DH_2O for continuous grinding. Finally, 0.025 mL of Triton × -100 was added as a dispersing agent followed by grinding well with the mixture for additional 30 minutes until the paste became homogeneous. The prepared paste was deposited near the top edge of FTO glass between the two pieces of the tape and then was coated by tape casting skill with a doctor blade [20–22]. This process was continued until the layer became uniform and smooth. The tape was removed with care without scratching the TiO_2 coating. Figure 2 shows the corresponding paste preparation procedures using biosynthesized TiO_2 NPs and its deposition on to the cleaned FTO glass substrate.

The as-prepared biosynthesized TiO_2 film was fired at 450°C in a muffle furnace for about 30 minutes to remove the organic solvents. This procedure also ensured electrical contact with good adhesion between the particle film and substrate.

2.6.3. Electrode Sensitization. Sensitizers obtained from roots of *Kniphofia schemperi* dye were adsorbed on top of TiO_2 photoelectrodes as follows. The TiO_2 film-coated electrode was immersed into the solutions of roots of *Kniphofia schemperi* (dye) until the films were fully soaked with the dye solution for about 12 hours (shown in Figure 3(a)). The TiO_2 film-coated substrates with the adsorbed molecules of dye were taken out and rinsed with the same solvent used in dye extraction (absolute ethanol) to remove the unadsorbed dyes from the surface of the TiO_2-photoanode [19].

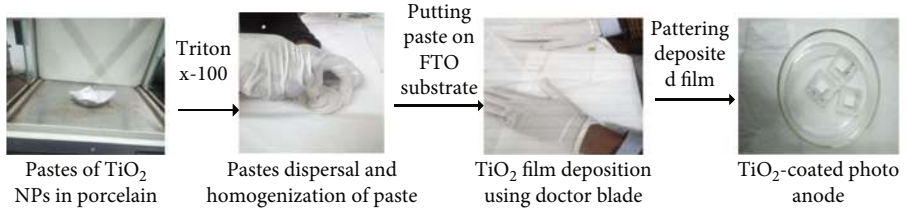

Figure 2: Flow charts for preparation of titanium oxide paste and its deposition as photoanode films on FTO glass substrate.

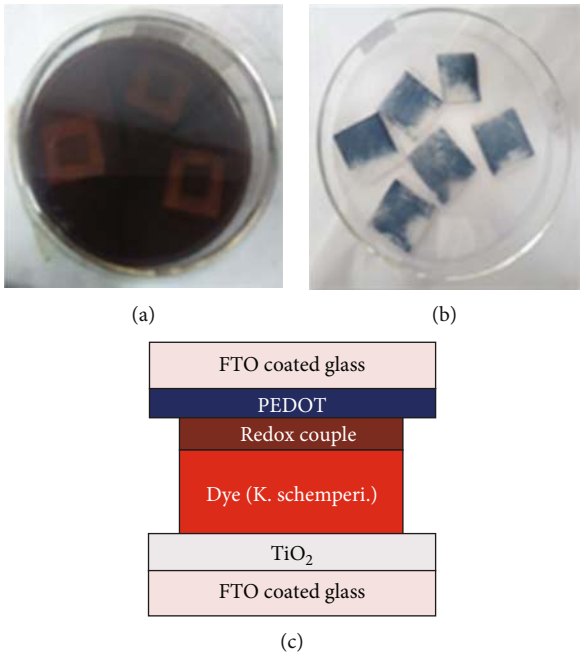

Figure 3: Pictures are showing (a) TiO_2-coated electrodes soaked into extracts of *K. schemperi*, (b) PEDOT-coated counter electrode, and (c) completed device structure of fabricated DSSCs.

2.6.4. Preparation of Redox Electrolytes. The polymer gel electrolyte was prepared according to the method developed by Fan et al. [23]. This was done by taking 4 mL 1-ethylene-3-methyl immidazolium iodide (EMIM-I) of 0.9 M and 25 mL acetonitrile, a high dielectric constant organic solvent, to form a homogeneous liquid electrolyte of 5.3 g under continuous stirring. In order to obtain a better conductivity, 0.5 M of sodium iodide was dissolved in the above homogeneous liquid electrolytes and then 0.12 M iodine and 35% (w/w) of polyvinyl pyrrolidone were added. Figure 4 reveals the formation of the quasisolid-state redox electrolyte from its components. The resulting mixture was heated at 70-80°C under vigorous stirring to dissolve the added PVP followed by cooling down to room temperature. Figure 4(b) with upside-down vial containing the redox electrolyte shows that the prepared electrolyte was really quasisolid (do not flow).

2.6.5. Coating the Counter Electrodes. The counter electrodes were prepared through electrochemical polymerization of 3, 4-ethylenedioxythiophene (EDOT) in a three-electrode cell by using an electrochemical analyzer. The electrochemical cell was consisted of FTO-spattered (conductive) glass substrate as the working electrode, a platinum foil as the counter electrode, and quasisilver/silver chloride as reference electrode. The solution/electrolyte system used for the preparation of counter electrode was performed by mixing 0.1 M EDOT and 0.1 M $(C_2H_5)_4NBF_4$ in acetonitrile solvent. The polymerization was carried out at a potential of +1.8 V for about 2 seconds through the bulk electrolysis with coulometer. At this potential, the electrode surface was covered with a blue-doped PEDOT film [24]. FTO glass substrates that were coated with PEDO counter electrode is shown in Figure 3(b), and then, completed device structures of the resulting DSSCs depicted in Figure 3(c) were ready for J-V and IPCE characterization.

2.6.6. Characterization of Fabricated DSSCs (J-V and IPCE). The current-voltage characteristics of fabricated solar cells were measured using a computer controlled electrochemical analyzer (CHI630A). A 250 W xenon lamp regulated by an Oriel Power Supply (Model 68830) was used to illuminate light on the DSSC samples. The intensity of the incident light was set at 100 mW·cm^{-2}. The DSSC solar cell was then mounted in a sample holder inside a metal box with an area of 1 cm^2 opening to allow light from the source. A grating

(a) (b)

Figure 4: (a) Upright and (b) inverted pictures of a vial containing prepared redox-electrolytes.

monochromator (Model 77250) was placed into the light path and used to select a wavelength between 300 and 800 nm with a 20-minute interval during measurement of incident photon to current conversion efficiency (IPCE).

3. Results and Discussion

3.1. Thermal Gravimetric and Differential Thermal Analysis (TGA-DTA). TGA-DTA was performed as a function of temperature as it can be shown in Figure 5. The analysis was done by taking 5.94 mg of the uncalcined biosynthesized TiO_2 (1 : 1) NP sample. The observed weight loss below 150°C was due to the evacuation of physically and chemically entangled water molecules from the surface of nanomaterials. In the temperature range of 150-355°C, the weight loss was also occurred due to the process of pyrolysis and carbonization of biomass materials from the synthesized TiO_2 NPs [25].

Weight loss was again observed and continued up to 483.15°C that was associated with a strong exothermic peak, which can be attributed to the vaporization of carbonized residues present over the surface of the biosynthesized nano-TiO_2. Similar result related to the present findings was also reported [12]. After 483.15°C-900°C, no considerable weight loss was observed as observed under the spectrum; therefore, 500°C was chosen as the calcination temperature for the biosynthesized TiO_2 NPs formed within three different volume ratios.

3.2. XRD Analysis. The crystalline nature of the biosynthesized TiO_2 NPs was analyzed using X-ray diffraction measurements. Figure 6 shows the XRD crystalline nature of the biosynthesized TiO_2 NPs formed within three different volume ratios. The diffraction peaks were observed at the 2θ values of ≈25.3, 38.0, 48.0, 53.2, 54.9, 62.7, 70.2, and 75.0, respectively, and along with their correspondence miller index values of (101), (004), (200), (105), (211), (204), (220), and (215), respectively. The diffraction peaks were found to be in a good agreement with JCPDS card number of 21-1272, which indicated the formation of the TiO_2 in the form of anatase. Diffraction peaks related to second phases were not observed, which confirmed that the biosynthesized TiO_2 NPs synthesized within 2 : 3, 1 : 1, and 3 : 2 ratios were pure.

The average crystalline sizes were calculated based on Debye Scherer's equation [12], and the values were found to be 11.7, 8.3, and 8.6 nm for 2 : 3, 1 : 1, and 3 : 2 volume ratios, respectively. Similar result related to the present study was also reported [26]. As compared to XRD result of TiO_2 (3 : 2) ratio, TiO_2 (1 : 1) ratio had a relatively smaller average crystalline size of ≈8.3 nm. This difference might be due to the fact that the excess amount of root extract added and used as a template to block the grain growth of TiO_2 (1 : 1) relative to the remaining two ratios of TiO_2 NPs. As it was observed from the XRD spectrum, TiO_2 (2 : 3) NP losses their crystalline nature due to the excessive addition of the root extract of *Kniphofia schemperi*. The excessive root extract with the polymer chain structure is difficult to completely burn out at 500°C; therefore, those residues on TiO_2 NPs block the diffraction signals with XRD analysis.

3.3. SEM-EDS Analysis. Morphology of the formed nanoparticles within three volume ratio of precursor salt and that of *Kniphofia schemperi* ethanolic root extract has been studied with the help of SEM-EDS. Figure 7 depicts the SEM images of TiO_2 NPs biosynthesized in the volume ratios of (a) 2 : 3, (b) 1 : 1, and (c) 3 : 2 and the corresponding EDS analysis of TiO_2 from the selected area in SEM image. From SEM images, the morphology of TiO_2 NPs was found to be spherical in shape with distinct edges. SEM image also revealed the increase in the particle size with the corresponding increase in the amount of ethanolic root extract of *Kniphofia schemperi* [27]. Agglomeration of the particles in Figure 7(a) is attributed because of the presence of excess amount of root extract [28]. To confirm and gather different information, a further insight about the biosynthesized TiO_2 nanoparticles formed within a volume ratio of 2 : 3, 1 : 1, and 3 : 2, analysis of the sample using EDS techniques was performed. It is necessary to verify the presence of desired elements in the biosynthesized TiO_2 NPs formed as 2 : 3, 1 : 1, and 3 : 2. The absence of any foreign materials in all of the three ratios indicates the high purity of our synthesized TiO_2 NPs [29].

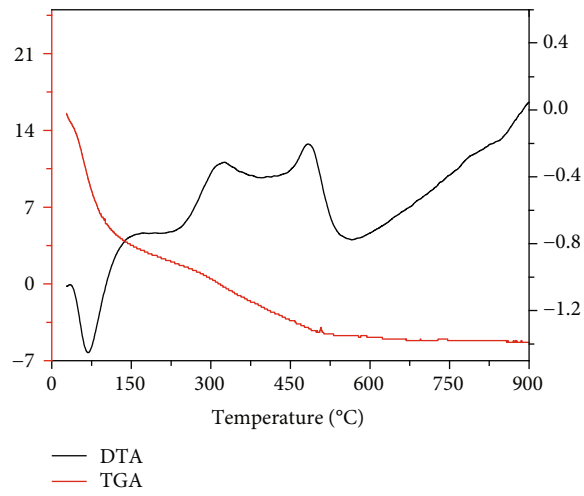

Figure 5: Thermal analysis results for the uncalcined TiO_2 (1 : 1) NPs.

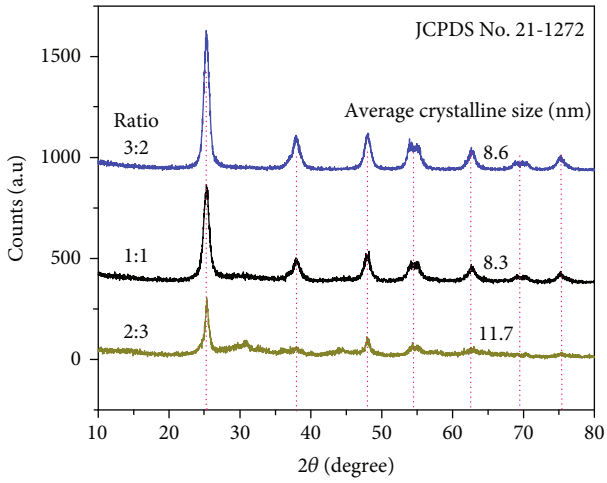

Figure 6: XRD spectra of biosynthesized TiO_2 NPs obtained using 0.25 M Ti precursor versus the root extract of *Kniphofia schemperi*.

3.4. TEM and SAED Analysis. In order to assure and get further information and insights about the feature of the TiO_2 NPs, TEM, HRTEM, and SAED analysis were carried out. Figure 8 shows TEM micrograph and the selected area electron diffraction (SAED) pattern as well as the correspondence high-resolution transmission electron microscope (HRTEM) image of TiO_2 (1 : 1) NPs. The image showed the nanoparticles of ~10 nm in size as also supported by the result of XRD analysis. The SAED pattern with circular rings for (101), (004), (200), (105), (211), (204), (220), and (215) planes indicated the polycrystalline nature of *Kniphofia schemperi* root mediated synthesized TiO_2, as supported by the XRD analysis results [12].

The image in Figure 8(c) showed HRTEM of anatase TiO_2 NPs. A fringe width of 0.355 nm Figure 8(b) in particle demonstrates for the (101) plane of anatase biosynthesized TiO_2 NPs. The lattice fringes also display the nanocrystalline nature of the biosynthesized TiO_2 NP anatase phase form.

3.5. UV-Vis Absorbance and Tauc Plot Analysis. Figure 9(a) shows the UV-Vis absorption spectra of TiO_2 NPs prepared at different volume ratios of 2 : 3, 1 : 1, and 3 : 2 in terms of the 0.25 Ti precursor salt and root extract of *Kniphofia schemperi*. The absorbance of TiO_2 NPs showed spectral shift for TiO_2 NPs at different precursor ratios. Compared to the very low absorption of the reference TiO_2 NPs, our TiO_2 NPs biosynthesized at different volume ratios exhibited a slight shift of the absorption edge towards the visible region due to their smaller size. The energy bandgaps of the biosynthesized TiO_2 NPs were estimated using the Tauc's plot method technique [15]. With the Tauc plot in terms of the $(\alpha h\nu)^2$ versus $h\nu$ in Figure 9(b), the energy bandgaps (E_g)f TiO_2 NPs were determined to be 3.35, 3.33, and 3.36 eV for the different volume ratios of TiO_2 synthesized within a volume ratio of 2 : 3, 1 : 1, and 3 : 2, respectively. The slight variation in E_g for TiO_2 NPs is due to the variation in volume ratio between Ti precursor salt and the root extract of *Kniphofia schemperi* that results in light absorption at different UV-Vis regions of absorption.

3.6. Functional Group Analysis Using FTIR. Fourier transformation infrared spectroscopy analysis was done to identify and confirm the role of biomolecules that was responsible for capping and reducing of the bioreduction of TiO_2 NPs. Figure 10 displays the FTIR spectra analysis of root powder of *Kniphofia schemperi* (a), calcined biosynthesized TiO_2 NPs (b), and uncalcined biosynthesized TiO_2 NPs (c). Figure 10(a) shows the FTIR spectrum of root powder and the peaks located at 3409.81, 2922.63, 2840.53, 2327.02, 1620.65, 1387.52, and 1065.32 cm^{-1}. The bands centered at 3409.81 cm^{-1} are attributed to ?-H_2O bending and vibration of hydroxyl groups present in the root of *Kniphofia schemperi*. This peak also refers to the H-bonded alcohols and phenolic compounds. These bonds are related to the chemical composition of root of *Kniphofia schemperi*. The week bands found at around 2922.63 and 2840.53 cm^{-1} represents H-C-H and -C-H groups associated by H-bond. The peaks appeared in the region of 1620.65 cm^{-1} are ascribed to the C=O bond of aromatic rings present in the root of *Kniphofia schemperi*. This region also relates to O-C-O asymmetric and symmetric stretching of carboxylic acids and can be attributed to the stretching of hydroxyl and water molecules too.

The peak presented around 1620.65 cm^{-1} could also represent the C=C bond of saturated hydrocarbons. The characteristic peaks of 1387.52 represents the C-H rock alkenes, while the peak observed at around 1065.32 cm^{-1} indicates the presence of C-O stretching alcohols, carboxylic acids, esters, and ethers. This peak may also depict the existence of aliphatic amines [30].

Figure 10(b) showed the FTIR spectrum of calcined biosynthesized titanium oxide nanoparticles, and the peaks are observed at around 3422.97, 2327.02, 1634.60, 1380.55, and 551.81 cm^{-1}. The broad absorption peak observed at 3422.97 cm^{-1} represents the presence of Ti-OH bonds. The characteristic peak shown at 2327.02 cm^{-1} indicates the alkene group with C=H stretching. The medium absorption peak at 1634.60 cm^{-1} represents the C=O stretching of primary amide

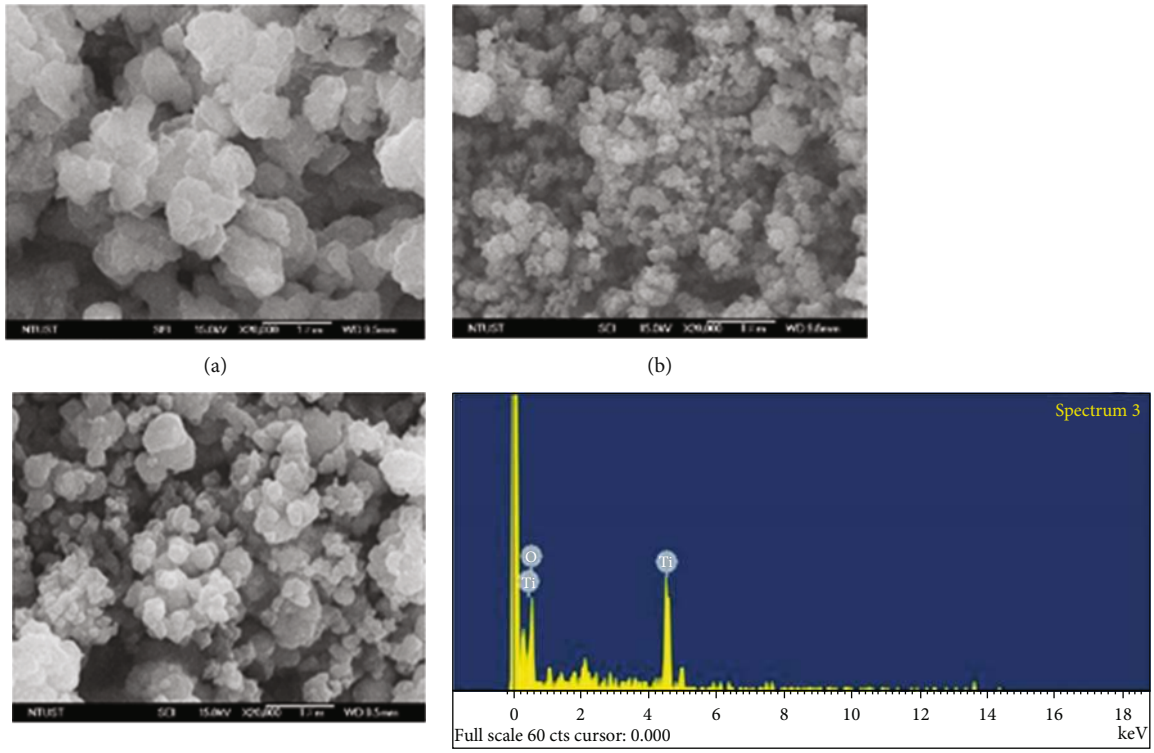

FIGURE 7: SEM images of TiO_2 NPs biosynthesized with the volume ratios of (a) 2 : 3, (b) 1 : 1, (c) 3 : 2, and (d) EDS spectrum of TiO_2 (1 : 1) NPs.

or to C=C groups of aromatic rings that plays as stabilizer and reducing agents during the stage of synthesis. This band also relate to the bending mode of vibration of O-H group and flavones. The peak represented by 1380.55 cm^{-1} refers to the aromatic ethers of C-O stretching and also the C-H rock like alkene groups. Peaks of C=O and C=C clearly indicates the presence of biomolecules and bioactive constituents from roots of *Kniphofia schemperi* extract that was used as a capping and reducing agent during the synthesis process of TiO_2 NPs within different volume ratios. The peak at 551.81 cm^{-1} is indicating the presence of Ti-O stretching vibration, and this confirms the formation of metal-oxygen bonding [31]. The analysis confirms the formation of TiO_2 with many surface hydroxyl function groups. The extra peaks from the organic C and O bonds are attributed to a trace amount of extract pyrolytic residues left after a relatively lower temperature firing procedure. These results indicated that the presence of alcohols, phenols, primary amines, ketones, and aliphatic amines in the root extract of *Kniphofia schemperi* that have been participated in the process of synthesis of TiO_2 NPs is responsible for the bioreduction of $TiO(OH)_2$ to TiO_2 NPs [30].

As it can be depicted under Figure 10(c), the peaks observed at 3409.81, 2922.63, 2320.05, 1620.65 1319.36, 1038.21, and 777.97 cm^{-1} represent O-H bond stretching due to adsorbed moisture, the CH, CH_2, and CH_3 functional groups linked via H- bonds, C=O bond stretching that might be due to the presence of adsorbed carbon dioxide on the surface of TiO_2, the surface water and hydroxyl groups, the C-H of alkenes, and the C-O bond of stretching of alcohols, carboxylic acids, ethers, and esters, respectively. In addition to this, the FTIR analysis indicated in Figure 9(c) shows the broad band centered at round 777.97 cm^{-1} which represents a characteristic peak to be believed due to the interaction of the biosynthesized nanooxide with biomolecules of the extract. As compared to the FTIR spectra of root powder and uncalcined TiO_2 NPs, the absence of different functional groups located at around 2922.63, 2840.53, and 1038.21 cm^{-1} in the calcined biosynthesized TiO_2 NPs confirms that these functional groups were eliminated during the firing process. Therefore, this characterization technique provides information as the extract plays great role and removed after calcination process was carried out [31].

3.7. Absorption Spectra of Root Extract of Kniphofia schemperi Sensitizer. Figure 11 reveals the corresponding optical absorption spectra of root of *Kniphofia schemperi* natural sensitizer. The roots of *Kniphofia schemperi* sensitizer show a strong absorption band at around 231 nm. The absorption of *Kniphofia schemperi* ascribes to the component, namely, anthocyanin, a group of natural phenolic compounds [32]. This result confirms that the pigment extracted from this natural dye can be used as a photosensitizer because it strongly absorbs photons in a wide UV-Vis region of electromagnetic radiation. One of the essential requirements for photosensitizer with the best performance is to have the broad and intense absorption in the UV-Vis and near-IR regions of the solar spectrum.

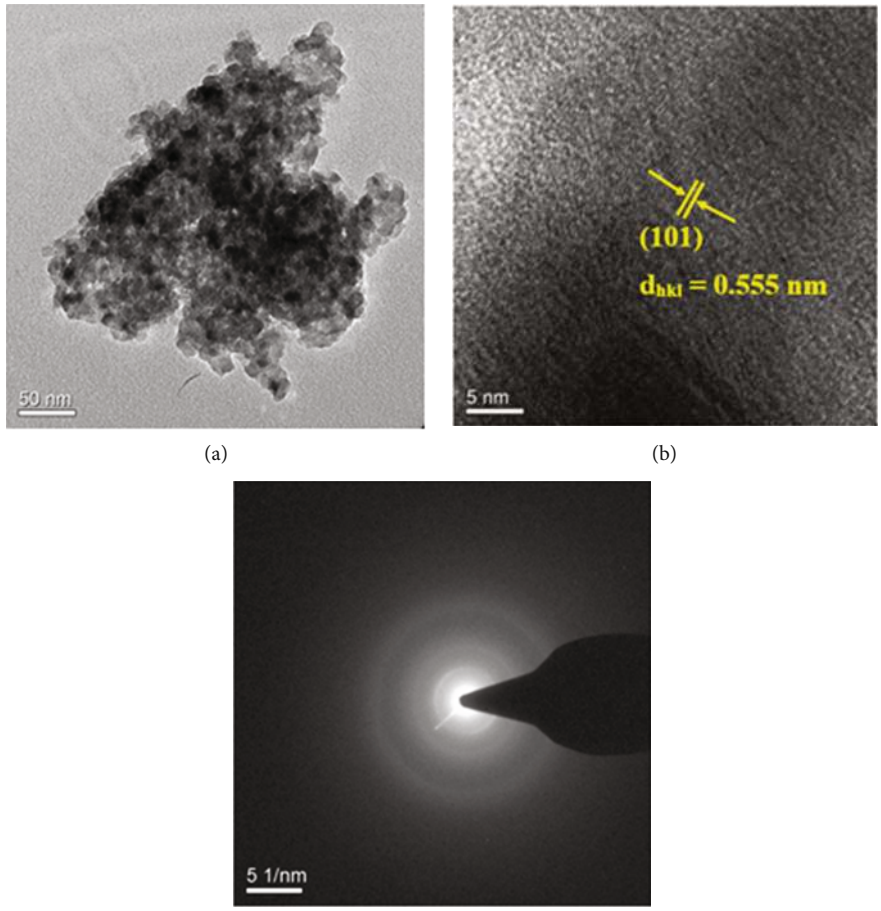

Figure 8: (a) TEM micrograph at 50 nm scale, (b) HRTM image, and (c) SAED pattern of TiO_2 (1 : 1) NPs.

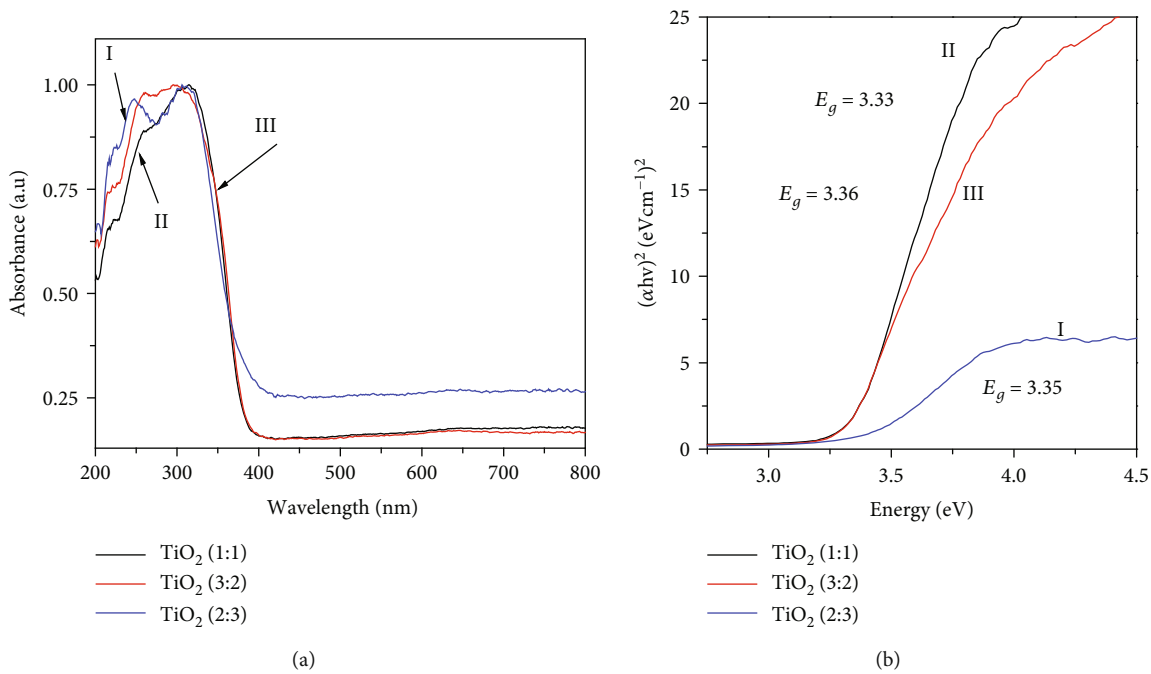

Figure 9: UV-Vis spectra (a) and Tauc plot of TiO_2 NPs (b) with (I) 2 : 3, (II) 1 : 1, and (III) 3 : 2 precursor volume ratios.

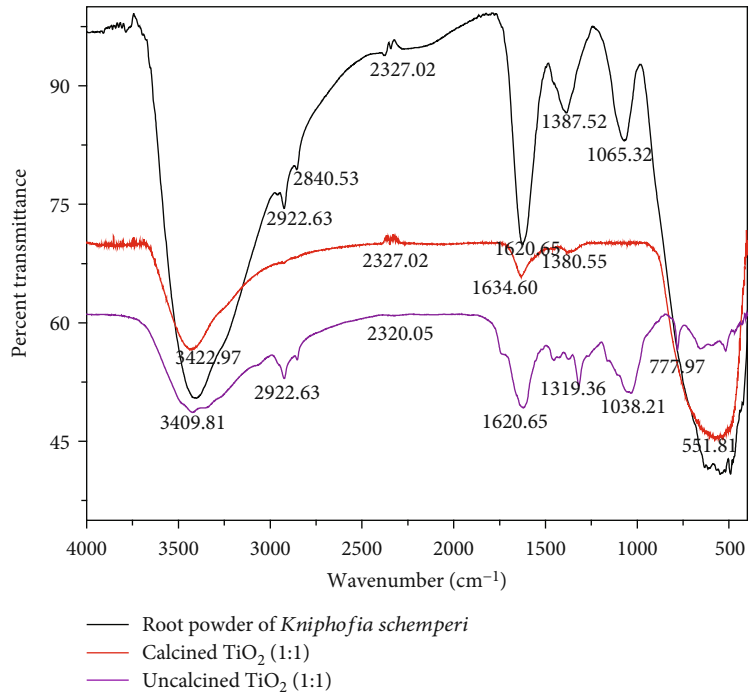

Figure 10: FT-IR spectra of root powder of *Kniphofia schemperi* (a), calcined TiO_2 (1 : 1) (b), and uncalcined TiO_2 (1 : 1) (c) NPs.

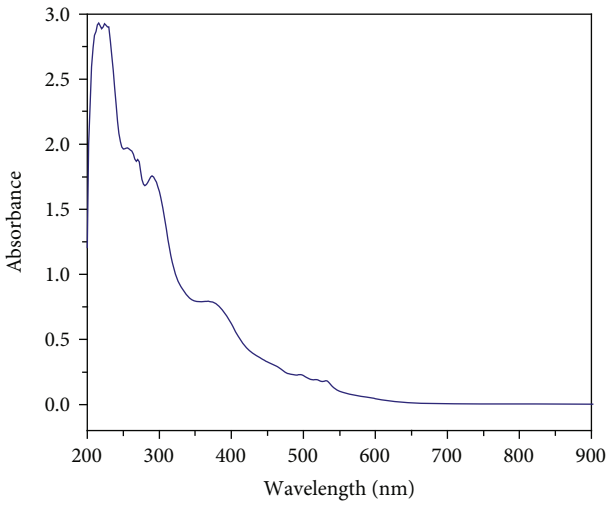

Figure 11: Optical absorption spectra of root of *Kniphofia schemperi* sensitizer.

3.8. Current Density-Voltage Characteristics of TiO_2-Based DSSCs. The photovoltaic tests of DSSCs prepared with a natural sensitizer extracted from roots of *Kniphofia schemperi* were performed by measuring the current density-voltage (J-V) characteristic curves by using Oriel Class Solar Simulator under the standard light intensity of illumination at 100 mW/cm^2. The performance of the DSSCs prepared using different volume ratio of biosynthesized TiO_2 NPs and the roots of *Kniphofia schemperi* sensitizer were evaluated by different parameters such as short circuit current density (J_{SC}), incident photon to current efficiency also known as quantum efficiency (η), open circuit voltage (V_{OC}), and fill factor (FF).

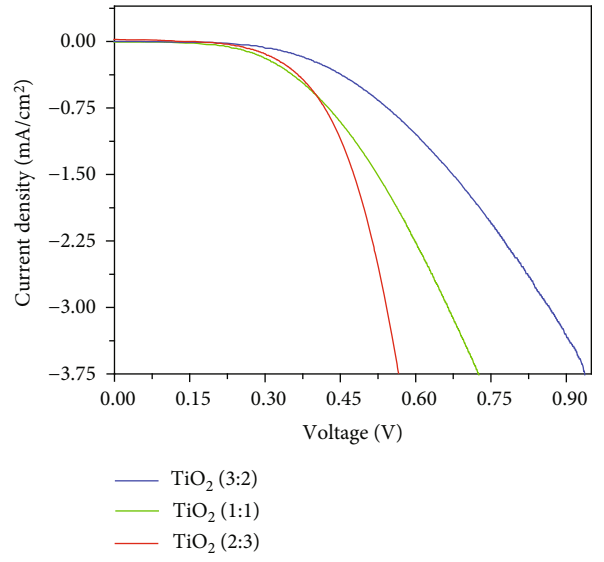

Figure 12: J-V curves of root of *Kniphofia schemperi* dye-filled DSSCs using biosynthesized TiO_2 NPs in volume ratios of (a) 2 : 3, (b) 1 : 1, and (c) 3 : 2.

Figure 12 shows the J-V curves of root of *Kniphofia schemperi*-based DSSCs prepared using TiO_2 photoanode at different precursor ratios. The compiled data from the J-V curves were presented in Table 1. The solar cell with TiO_2 (3 : 2) biosynthesized photoelectrodes shows the highest η value of 1.3%, the highest V_{OC} of 161 mV, the highest J_{SC} of 2.46×10^{-2} mA/cm^2, and slightly lower FF of 32.8%. The improvement in J_{SC} value of TiO_2 (3 : 2)-based DSSC is basically due to the improved absorption of light caused by the

Table 1: DSSC data of the different volume ratios of TiO_2 NPs.

TiO_2 ratio	J_{SC} (mA/cm^2)	V_{OC} (mV)	J_{max} (mA/cm^2)	V_{max} (mV)	P_{max} (mW/cm^2)	FF %	η%
2 : 3	1.29×10^{-3}	63	8.97×10^{-4}	38	3.41×10^{-2}	42	0.034
1 : 1	6.05×10^{-3}	48	4.17×10^{-3}	28	1.17×10^{-1}	40.3	0.117
3 : 2	2.46×10^{-2}	161	1.84×10^{-2}	70.6	1.30	32.8	1.300

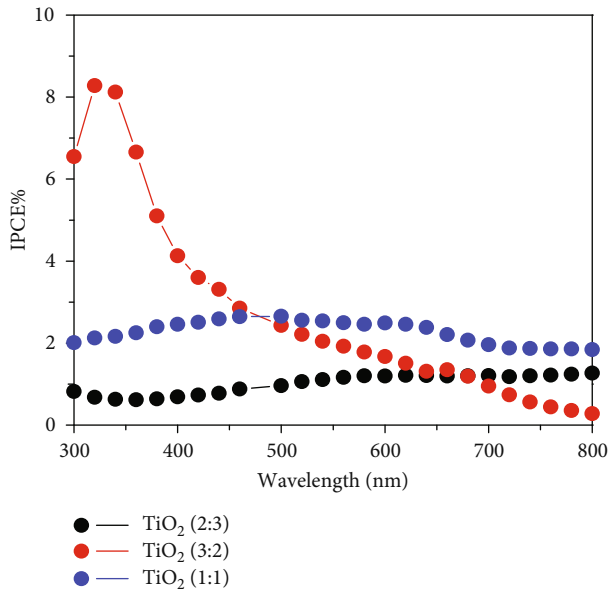

Figure 13: IPCE% spectra of DSSCs based on TiO_2 NPs in (a) 2 : 3, (b) 1 : 1, and (c) 3 : 2 ratios using root of *Kniphofia schemperi* as a light sensitizer.

wider range of absorption of sensitizer adsorbed on nanoparticles, as supported with Figure 12, while the enhanced efficiency attributed due to the improved crystallinity and morphological nature of TiO_2 photoelectrodes to allow more dye adsorption on its surface, larger band gap energy, and higher interaction between TiO_2 nanocrystalline film and the root extract of the sensitizer for better charge transfer [33].

In general, the efficiencies of DSSCs not only depend on the molecular structure of the natural pigment but also depend strongly on the properties of the biosynthesized photoelectrodes such as crystallinity, morphology, and aggregation of the dye molecules [34]. It was earlier reported that the power conversion efficiency of most of the DSSCs made from natural dyes and some organic synthetic dyes suffers from the low open circuit voltage, which is also the case in the present study where the open circuit voltage ranged from 29 to 161 mV for the biosynthesized photoanode with the different precursor volume ratios.

3.9. IPCE Characteristics of Biosynthesized TiO_2-Based DSSCs. Photoaction spectra provide further insights on the photoelectrochemical performance of biosynthesized photoelectrodes with the presence of sensitizers. As it can be observed from Figure 13, relatively maximum IPCE% value was obtained using TiO_2 (3 : 2) in the presence of ethanolic root extract of *Kniphofia schemperi* sensitizer, and this value is 8.11%, which was located at a wavelength of 340 nm. The improvement in IPCE% value relative to the remaining photoelectrodes results from higher electron transportation at the electrolyte interfaces and good electrocatalytic activity of the photoelectrode [34]. Again, TiO_2 (1 : 1) with the presence of *Kniphofia schemperi* sensitizer possess an IPCE% of 2.66% which occurs at 500 nm. This action spectra response is contributed by sensitizer.

Low IPCE% value was recorded using biosynthesized photoelectrode obtained within a 2 : 3 ratio, and the value was estimated as 1.27% at a wavelength value of 800 nm. This low value of IPCE% may be attributed due to inefficient light harvesting efficiency (LHE) by the dye, that is, inefficient charge injection into the prepared TiO_2 film or inefficient collection of injected electrons [35].

For devices of DSSCs (with 2 : 3 volume ration of TiO_2 film), the IPCE values of 1~2% were recorded at 500-800 nm as shown in Figure 13, while negligibly small amount of absorption was observed for the film (Figure 9(a)). The IPCE value of DSSCs depends not only on the light-absorbing nature of semiconductor (TiO_2 NPs) but also on light absorption of sensitizer (dye), absorption and interaction of redox electrolyte, and the interaction of dye molecules with TiO_2 film.

According to previous reports [36–38], the redox couple (quasisolid-state electrolyte) involves in light absorption (in certain amount) in visible region even beyond 500 nm and has a contribution for IPCE values. The films of photoanode of TiO_2 NPs (with anatase phase structure) are highly porous. These porous structures of TiO_2 NPs provide larger surface area for anchoring of dye molecules [39, 40]. Light-absorbing dye molecules attached to the semiconductor (TiO_2 NPs) through their functional groups such as carboxylic acid, phenol, and flavonoids interact with titanium metal as ligand in the film. As of some other reports [41], the ligand-metal (push-pull) type of interaction established between dye molecule and TiO_2 NPs contributes for significant charge separation, minimizes electron-hole recombination, and minimizes series resistance between semiconductor (TiO_2 NPs) and light sensitizer that confirms the higher efficiency of photon-to-electron conversion or incident photon to current conversion efficiency (IPCE%).

4. Conclusion

In conclusion, TiO_2 NPs had been successfully biosynthesized using titanium tetra butoxide precursor salt and *Kniphofia schemperi* root extract at different volume ratios. The biosynthesized NPs were thermally stable above 500°C. XRD

analysis proved that the average particle size of the synthesized TiO_2 NPs was found in the range of 8.3-11.7 nm. SEM-EDS revealed morphology of the biosynthesized TiO_2 NPs to be spherical and the composition with only the elements of Ti and O. The calculated bandgap energies were in the range of 3.33-3.36 eV. Functional group analysis indicated the presence of a trace amount of extract pyrolytic residues left. Among the TiO_2 NPs biosynthesized at different precursor ratios, the best solar cell conversion to electricity was obtained for *Kniphofia schemperi*-based dye-filled DSSC using TiO_2 (3 : 2) photoelectrodes which was estimated as 1.3%.

Data Availability

The research data used to support the findings of this study are included in the article.

Conflicts of Interest

The authors fully declare that they have no conflicts of interest.

Acknowledgments

The authors highly acknowledged Adama Science and Technology University (ASTU) for funding this research work through ASTU's 12th cycle research grant effectively. The authors offer their gratitude to the Department of Materials Science and Engineering at Adama Science and Technology University for allowing facilities such as thermal analyzer and XRD. Department of Chemistry at Addis Ababa University was also thanked by authors for allowing FT-IR analysis and computer controlled electrochemical analyzer (CHI630A).

References

[1] Y. Fang, P. Ma, H. Cheng et al., "Synthesis of low-viscosity ionic liquids for application in dye-sensitized solar cells," *Asian Journal of Chemistry*, vol. 14, no. 23, pp. 4201–4206, 2019.

[2] J. Gong, J. Liang, and K. Sumathy, "Review on dye-sensitized solar cells (DSSCs): fundamental concepts and novel materials," *Renewable and Sustainable Energy Reviews*, vol. 16, no. 8, pp. 5848–5860, 2012.

[3] B. O'Regan and M. Grätzel, "A low-cost, high-efficiency solar cell based on dye-sensitized colloidal TiO_2 films," *Nature*, vol. 353, no. 6346, pp. 737–740, 1991.

[4] R. Jose, V. Thavasi, and S. Ramakrishna, "Metal oxides for dye-sensitized solar cells," *Journal of the American Ceramic Society*, vol. 92, no. 2, pp. 289–301, 2009.

[5] L. Rodríguez-Sánchez, M. C. Blanco, and M. A. López-Quintela, "Electrochemical synthesis of silver nanoparticles," *Journal of Physical Chemistry B*, vol. 104, no. 41, pp. 9683–9688, 2000.

[6] S. Ahmed, Saifullah, M. Ahmad, B. L. Swami, and S. Ikram, "Green synthesis of silver nanoparticles usingAzadirachta indicaaqueous leaf extract," *Journal of Radiation Research and Applied Science*, vol. 9, no. 1, pp. 1–7, 2016.

[7] E. d'Avigdor, H. Wohlmuth, Z. Asfaw, and T. Awas, "The current status of knowledge of herbal medicine and medicinal plants in Fiche, Ethiopia," *Journal of Ethnobiology and Ethnomedicine*, vol. 10, no. 1, p. 38, 2014.

[8] E. T. Bekele, B. A. Gonfa, O. A. Zelekew, H. H. Belay, and F. K. Sabir, "Synthesis of titanium oxide nanoparticles using root extract of *kniphofia foliosa* as a template, characterization, and its application on drug resistance bacteria," *Journal of Nanomaterials*, vol. 2020, Article ID 2817037, 10 pages, 2020.

[9] J. Y. Liao, B. X. Lei, D. B. Kuang, and C. Y. Su, "Tri-functional hierarchical TiO_2 spheres consisting of anatase nanorods and nanoparticles for high efficiency dye-sensitized solar cells," *Energy and Environmental Science*, vol. 4, no. 10, pp. 4079–4085, 2011.

[10] T. Santhoshkumar, A. A. Rahuman, C. Jayaseelan et al., "Green synthesis of titanium dioxide nanoparticles using _Psidium guajava_ extract and its antibacterial and antioxidant properties," *Asian Pacific Journal of Tropical Medicine*, vol. 7, no. 12, pp. 968–976, 2014.

[11] D. Ramimoghadam, M. Z. B. Hussein, and Y. H. Taufiq-Yap, "Hydrothermal synthesis of zinc oxide nanoparticles using rice as soft biotemplate," *Chemistry Centeral Journal*, vol. 7, no. 1, 2013.

[12] J. Xu, L. Li, Y. Yan et al., "Synthesis and photoluminescence of well-dispersible anatase TiO_2 nanoparticles," *Journal of Colloid and Interface Science*, vol. 318, no. 1, pp. 29–34, 2008.

[13] P. Pookmanee, H. Ninsonti, S. Sangsrichan, W. Kangwansupamomkon, and S. Phanichphant, "Photocatalytic degradation of geosmin by titanium dioxide powder synthesized by the hydrothermal route," *Advanced Materials Research*, vol. 93-94, pp. 161–164, 2010.

[14] E. Figgemeier, W. Kylberg, E. Constable et al., "Titanium dioxide nanoparticles prepared by laser pyrolysis: synthesis and photocatalytic properties," *Applied Surface Science*, vol. 254, no. 4, pp. 1037–1041, 2007.

[15] M. Kolenčík, D. Ernst, M. Urík et al., "Foliar application of low concentrations of titanium dioxide and zinc oxide nanoparticles to the common sunflower under field conditions," *Nanomaterials*, vol. 10, no. 8, p. 1619, 2020.

[16] C. Das, S. Sen, T. Singh et al., "Green synthesis, characterization and application of natural product coated magnetite nanoparticles for wastewater treatment," *Nanomaterials*, vol. 10, no. 8, p. 1615, 2020.

[17] K. Uma, E. Muniranthinam, S. Chong, T. C.-K. Yang, and J.-H. Lin, "Fabrication of hybrid catalyst ZnO $_{\text{Nanorod/α-Fe2O3}}$ composites for hydrogen evolution reaction," *Crystals*, vol. 10, no. 5, p. 356, 2020.

[18] D. J. Godibo, S. T. Anshebo, and T. Y. Anshebo, "Dye sensitized solar cells using natural pigments from five plants and quasi-solid state electrolyte," *Journal of the Brazilians Chemical Society*, vol. 26, no. 1, pp. 92–101, 2015.

[19] M. K. Nazeeruddin, A. Kay, I. Rodicio et al., "Conversion of light to electricity by cis-X2bis(2,2′-bipyridyl-4,4′-dicarboxylate)ruthenium(II) charge-transfer sensitizers (X = Cl-, Br-, I-, CN-, and SCN-) on nanocrystalline titanium dioxide electrodes," *Journal of American Chemical Society*, vol. 115, no. 14, pp. 6382–6390, 1993.

[20] S. S. Shenouda, I. S. Yahia, H. S. Hafez, and F. Yakuphanoglu, "Facile and low-cost synthesis of PEDOT: PSS/FTO polymeric counter electrode for DSSC photosensor with negative capacitance phenomenon," *Materials Research Express*, vol. 6, no. 6, article 065004, 2019.

[21] R. Ghayoor, A. Keshavarz, M. N. S. Rad, and A. Mashreghi, "Enhancement of photovoltaic performance of dye-sensitized solar cells based on TiO_2-graphene quantum dots photoanode," *Materials Research Express*, vol. 6, no. 2, article 025505, 2019.

[22] M. Shang, B. Liu, Z. Dong, Z. Dong, and L. Dong, "Effects of counter electrodes on photovoltaic performance of all-solid-state TiO_2-based dye-sensitized solar cells," *Materials Research Express*, vol. 2, no. 3, article 035502, 2015.

[23] L. Fan, S. Kang, J. Wu, Z. Lan, and J. Lin, "Quasi-solid state dye-sensitized solar cells based on polyvinylpyrrolidone with ionic liquid," *Energy Sources, Part A:Recovery,Utilization, and Environmental Effects*, vol. 32, no. 16, pp. 1559–1568, 2010.

[24] C. H. Hong, H. S. Ko, E. M. Han, and K. H. Park, "Electrochemical properties of electrodeposited PEDOT counter electrode for dye-sensitized solar cells," *International Journal of Electrochemical Science*, vol. 10, no. 7, pp. 5521–5529, 2015.

[25] K. G. Rao, C. H. Ashok, K. V. Rao, C. G. S. Hakra, and V. Ajendar, "Synthesis of TiO_2 nanoparticles from orange fruit waste," *International Journal of Multidisciplinary Advanced Research Trends*, vol. 2, no. 1, pp. 2349–7408, 2015.

[26] A. Maurya, P. Chauhan, A. Mishra, and A. K. Pandey, "Surface functionalization of TiO_2 with plant extracts and their combined antimicrobial activities against E. faecalis and E. coli," *Journal of Research Updates in Polymer Science*, vol. 1, no. 1, pp. 43–51, 2012.

[27] M. M. Ba-Abbad, A. A. H. Kadhum, A. B. Mohamad, M. S. Takriff, and K. Sopian, "Synthesis and catalytic activity of TiO_2 nanoparticles for photochemical oxidation of concentrated chlorophenols under direct solar radiation," *International Journal of Electrochemical Science*, vol. 7, no. 6, pp. 4871–4888, 2012.

[28] C. Malarkodi, K. Chitra, S. Rajeshkumar et al., "Novel eco-friendly synthesis of titanium oxide nanoparticles by using Planomicrobium sp. and its antimicrobial evaluation," *Der Pharmacia Sinica*, vol. 4, no. 3, pp. 59–66, 2013.

[29] M. A. M. Al-Alwani, "Natural dye extracted from *Pandannus amaryllifolius* leaves as sensitizer in fabrication of dye sensitized solar cells," *International Journal of Electrochemical Science*, vol. 12, no. 1, pp. 747–761, 2017.

[30] D. C. L. Vasconcelos, V. C. Costa, E. H. M. Nunes, A. C. S. Sabioni, M. Gasparon, and W. L. Vasconcelos, "Infrared spectroscopy of titania sol-gel coatings on 316L stainless steel," *Materials Science and Applications*, vol. 2, no. 10, pp. 1375–1382, 2011.

[31] L. Andrea, R. Patricia, G. Carolina et al., "FTIR and raman characterization of TiO_2 nanoparticles coated with polyethylene glycol as carrier for 2-methoxyestradio," *Applied Sciences*, vol. 7, no. 1, 2017.

[32] S. Lucioli, C. Di Bari, C. Forni et al., "Anthocyanic pigments from elicited _in vitro_ grown shoot cultures of _Vaccinium corymbosum_ L., cv. Brigitta Blue, as photosensitizer in natural dye-sensitized solar cells (NDSSC)," *Journal of Photochemistry and Photobiology B: Biology*, vol. 188, pp. 69–76, 2018.

[33] W. Maiaugree, S. Lowpa, M. Towannang et al., "A dye sensitized solar cell using natural counter electrode and natural dye derived from *mangosteen* peel waste," *Scintifc Report*, vol. 13, no. 5, article 15230, 2015.

[34] H. Yu, S. Zhang, H. Zhao, G. Will, and P. Liu, "An efficient and low-cost TiO_2 compact layer for performance improvement of dye-sensitized solar cells," *Electrochemical Acta*, vol. 54, no. 4, pp. 1319–1324, 2009.

[35] E. Jonathan, M. Y. Onimisi, and D. Eli, "Natural pigments as sensitizers for dye sensitized solar cells," *Advances in Materials*, vol. 5, no. 5, pp. 31–34, 2016.

[36] Z. Yu, H. Tian, E. Gabrielsson et al., "Tetrathiafulvalene as a one-electron iodine-free organic redox mediator in electrolytes for dye-sensitized solar cells," *RSC Advances*, vol. 2, no. 3, pp. 1083–1087, 2012.

[37] J. F. Lu, J. Bai, X. B. Xu et al., "Alternate redox electrolytes in dye-sensitized solar cellsAlternate redox electrolytes in dye-sensitized solar cells," *Chinese Science Bulletin*, vol. 57, no. 32, pp. 4131–4142, 2012.

[38] H. Tian, Z. Yu, A. Hagfeldt, L. Kloo, and L. Sun, "Organic redox couples and organic counter electrode for efficient organic dye-sensitized solar cells," *Journal of the American Chemical Society*, vol. 133, no. 24, pp. 9413–9422, 2011.

[39] C. Cavallo, F. D. Pascasio, A. Latini, M. Bonomo, and D. Dini, "Nanostructured semiconductor materials for dye-sensitized solar cells," *Journal of Nanomaterials*, vol. 2017, Article ID 5323164, 31 pages, 2017.

[40] C. A. Bignozzi, R. Argazzi, and R. Boaretto, "The role of transition metal complexes in dye sensitized solar devices," *Coordination Chemistry Reviews*, vol. 257, no. 9-10, pp. 1472–1492, 2013.

[41] K. R. Juganta, K. Supratik, and L. Jerzy, "Insight into the optoelectronic properties of designed solar cells efficient tetrahydroquinoline dye sensitizers on TiO_2 (101) surface: first principles approach," *Scientific Reports*, vol. 8, no. 1, 2018.